Chaotic mixing induced transitions in reaction–diffusion systems

Zoltán Neufeld and Peter H. Haynes
Department of Applied Mathematics and Theoretical Physics, University of Cambridge, Silver Street, Cambridge CB3 9EW, United Kingdom

Tamás Tél
Eötvös University, Department of Theoretical Physics, H-1518 Budapest, Hungary

(Received 6 November 2001; accepted 7 March 2002; published 20 May 2002)

We study the evolution of a localized perturbation in a chemical system with multiple homogeneous steady states, in the presence of stirring by a fluid flow. Two distinct regimes are found as the rate of stirring is varied relative to the rate of the chemical reaction. When the stirring is fast localized perturbations decay towards a spatially homogeneous state. When the stirring is slow (or fast reaction) localized perturbations propagate by advection in form of a filament with a roughly constant width and exponentially increasing length. The width of the filament depends on the stirring rate and reaction rate but is independent of the initial perturbation. We investigate this problem numerically in both closed and open flow systems and explain the results using a one-dimensional ''mean-strain'' model for the transverse profile of the filament that captures the interplay between the propagation of the reaction–diffusion front and the stretching due to chaotic advection. © *2002 American Institute of Physics.* [DOI: 10.1063/1.1476949]

The problem of chemical or biological activity in fluid flows has recently become an area of active research.[1–8] Apart from theoretical interest this problem has a number of industrial[9] and environmental[10,11] applications. One of the simplest manifestations of nonlinear behavior in reaction–diffusion systems is the possibility of travelling front solutions. In this paper we study the effect of chaotic mixing, by an unsteady laminar flow, in reaction–diffusion systems supporting front propagation.

I. INTRODUCTION

Let us consider N interacting chemical or biological components, with dimensionless concentrations $C_i(\mathbf{r},t), i=1,..,N$, advected by an incompressible fluid flow, $\mathbf{v}(\mathbf{r},t)$, that is assumed to be independent of the concentrations. The spatiotemporal dynamics of the fields is governed by the set of reaction–advection–diffusion equations

$$\frac{\partial}{\partial t}C_i+\mathbf{v}(\mathbf{r},t)\cdot\nabla C_i=\mathcal{F}_i(C_1,..,C_N;k_1,..,k_M)+\kappa\Delta C_i, \tag{1}$$

where the functions $\mathcal{F}_i$ describe the interactions between the different components. These may be chemical reactions or, in the case of biological populations (e.g., different plankton species), they may represent growth, grazing, reproduction, death, predation, etc.[12,13] The parameters k_i are the reaction rates characterizing the speed of the chemical or biological interactions and κ is the diffusivity, assumed to be the same for all components. We assume that the flow is laminar (smooth) and time-dependent implying chaotic advection,[14–16] i.e., fluid elements separate exponentially at a rate given by the Lyapunov exponent,[17] λ, of the advection dynamics.

Equation (1) can be nondimensionalized by the transformations

$$x\to\frac{x}{L},\quad t\to\frac{tU}{L},\quad v\to\frac{v}{U},\quad k_i\to\frac{k_i}{k_1},$$
$$\mathcal{F}_i(C_1,\ldots,C_N)\to\frac{\mathcal{F}_i(C_1,\ldots,C_N)}{k_1}, \tag{2}$$

where L and U are the characteristic length scale and velocity of the flow and one of the reaction rates, $k\equiv k_1$, is used to define a characteristic chemical time scale. Thus, the nondimensional problem can be written as

$$\frac{\partial}{\partial t}C_i+\mathbf{v}(\mathbf{r},t)\cdot\nabla C_i=\mathrm{Da}\,\mathcal{F}_i(C_1,\ldots,C_N)+\mathrm{Pe}^{-1}\Delta C_i, \tag{3}$$

where

$$\mathrm{Da}\equiv\frac{kL}{U}\quad\text{and}\quad\mathrm{Pe}\equiv\frac{LU}{\kappa} \tag{4}$$

are the Damköhler and the Péclet number, respectively. The Damköhler number,[18,19] Da, characterizes the ratio between the advective and the chemical (or biological) time scales. Large Da corresponds to slow stirring or equivalently fast chemical reactions and vice versa. The Péclet number, Pe, is a measure of the relative strength of advective and diffusive transport. We are going to consider the case of large Pe number, typical in many applications, when advective transport dominates except at very small scales.

In applications it may be useful to understand the behavior of a chemical system for a range of stirring speeds when other parameters (e.g., reaction rate constants, diffusivity) are kept unchanged. Although the stirring speed affects both nondimensional numbers in (4), its variation leaves the family of curves on the Da–Pe plane defined by DaPe = constant invariant. For this case the appropriate nondimen-

sional equation could be obtained by dividing both sides of (3) by Da, implying the use of the chemical time scale, $1/k$, as the time unit. Then the two nondimensional parameters would be Da and $\mathrm{DaPe}=kL^2/\kappa$, where the latter, representing the ratio of the diffusive and the chemical time scales, is independent of the stirring rate.

In this paper, we study the behavior of the chemical system for different Damköhler numbers, when the Péclet number is kept fixed. Strictly speaking, this corresponds to the variation of the chemical reaction rates and cannot be achieved by changing the stirring rate alone (except if the diffusivity is also changed in order to keep Pe constant).

For simplicity, in the following we consider the case of two-dimensional flow only, since it is computationally cheaper and easier to visualize. This is directly relevant to certain geophysical problems where density stratification makes the flow quasi-two-dimensional (e.g., stratospheric chemistry, plankton in the ocean surface layer) and is also accessible to laboratory experiments (using soap-films, stratified fluids, etc.). However we believe that many of the results presented in this paper can be straightforwardly extended to three-dimensional systems.

With the above assumptions the problem defined by Eq. (3) is still very general until the interaction terms, $\mathcal{F}_i$ are specified. Previous work has investigated the spatial structure of the chemical fields in the case of chemical dynamics with a single stable local equilibrium concentration, that is a function of the spatial coordinate.[20–23] Here we consider the case of chemical systems that in the spatially homogeneous case would have multiple steady state solutions. There are many examples of multiple steady states in interacting chemical or biological systems, in models of atmospheric chemistry,[24] or in the dynamics of plankton populations.[12,25] Perhaps the simplest is the autocatalytic reaction $A+B\rightarrow 2B$.

Thus we assume that the dynamical system that describes the evolution of the spatially uniform chemical system, $C_i(\mathbf{r},t)\equiv C_i(t)$,

$$\frac{dC_i}{dt}=\mathrm{Da}\,\mathcal{F}_i(C_1,..,C_N) \tag{5}$$

has more than one, stable or unstable, fixed point, or equivalently the system of equations

$$\mathcal{F}_i(C_1^*,\ldots,C_N^*)=0 \tag{6}$$

has multiple roots in the positive quadrant. (Since the concentration fields must be positive everywhere, only the fixed points with $C_i^*\geqslant 0$ are relevant.)

We study the response of the system, initially in one of the uniform steady states, to a localized perturbation. By localized we mean, that the the spatial extent of the perturbation, δ, is much smaller than the characteristic length scale of the velocity field, $\delta\ll 1$. The evolution of the chemical fields is investigated for different values of the Damköhler number in both closed flow and open flow systems. The cases of stable and unstable initial uniform states will be considered separately, each represented by a simple model system.

In the following section we describe the models used for the reaction dynamics and for the flow, followed by the presentation of explicit two-dimensional numerical simulations in Sec. III. Then, in Sec. IV we introduce and investigate a one-dimensional reduced model and show that this may be used successfully to interpret the two-dimensional numerical simulations. The paper ends with a summary and discussion.

II. THE MODELS

For the reaction term, $\mathcal{F}$, we use two different models with multiple equilibria with quadratic and cubic nonlinearity. The first is an autocatalytic reaction, a generic model for the propagation of a stable phase into an unstable one. The second model is a bistable system and we study the triggering of a transition from one stable state to the other by a localized perturbation.

(1) **Autocatalytic reaction**—Let us consider the reaction $A+B\rightarrow 2B$, with the corresponding rate equations for the spatially uniform system

$$\frac{dC_A}{dt}=-rC_AC_B,\quad \frac{dC_B}{dt}=rC_AC_B. \tag{7}$$

Observing that C_A+C_B (the total number of molecules A and B) is conserved by the reaction, we can eliminate C_A and characterize the state of the system with a new variable $C\equiv C_B/(C_A+C_B)$ $(0<C<1)$ representing the proportion of component B, that evolves according to

$$\frac{dC}{dt}=k\mathcal{F}(C)\equiv kC(1-C), \tag{8}$$

where $k=r(C_A+C_B)$.

There are two steady states: (i) $C=0$ (component A only). This is unstable, since the addition of a small amount of B leads to the complete consumption of A through the autocatalytic reaction; (ii) $C=1$ (component B only). This is stable—a small amount of A is quickly transformed back to B.

The temporal evolution of the spatially homogeneous system can be obtained by integrating (8) as

$$C(t)=\left[1+\left(\frac{1-C(0)}{C(0)}\right)e^{-kt}\right]^{-1}, \tag{9}$$

where $C(0)$ is the initial proportion of component B.

In the numerical experiments, the initial state is the unstable phase, $C=0$, perturbed by a localized pulse of the form

$$C(x,y,t=0)=C_0e^{-(x^2+y^2)/2\delta^2}, \tag{10}$$

where $C_0\ll 1$ and $\delta\ll 1$, representing a small dilute patch of the catalyst, component B.

The reaction term (8) can also be interpreted as the, so-called, logistic growth of a population[26] modelling the growth of the population limited by the availability of the resources (e.g., nutrients), implying that the concentration saturates at $C=1$. Furthermore, the same reaction term appears in the Kolmogorov–Piskunov–Petrovsky (KPP) equation[27] used in combustion,[9,28] which describes the propagation of a flame front separating fresh (unburned) pre-

mixed reactants ($C=0$) and burned gases ($C=1$). Thus our numerical experiments can also be regarded as representing the evolution of a plankton bloom stirred by ocean currents or of a flame embedded in a laminar flow.

(2) **Bi-stable system**—As a second model we use a system with two stable states defined by the reaction equation

$$\frac{dC}{dt}=k\mathcal{F}(C)=kC(\alpha-C)(C-1), \quad 0<\alpha<1. \tag{11}$$

The stable fixed points are $C=0$ and $C=1$, and their basins of attraction are separated by the unstable fixed point, $C=\alpha$. Although this system does not represent a real chemical reaction scheme, it is the simplest possible model for multistability. We expect that more realistic chemical and biological systems with multiple stable steady states would show similar behavior. We start the system in the stable uniform state, $C=0$, and a localized perturbation of the form (10) is added. Now the amplitude of the perturbation is chosen such to exceed the threshold, α (we use $C_0=1.0$). [Since the initial state is stable, any perturbation that is below the threshold everywhere, $C(x,0)<\alpha$, dies out.]

We note that when $C=\alpha$ is chosen as an initial state the bistable model shows qualitatively similar behavior to the autocatalytic model.

Stirring will be modelled by two simple time-periodic model velocity fields, representing a closed and an open flow system, respectively. We stress, however, that the results described in this paper are valid for a wide class of two-dimensional time-dependent laminar flows, since the only important assumption is the chaotic motion of fluid elements.

For the closed flow we choose a sinusoidal shear flow with the direction of the shear periodically alternating along the x and y axis.[29,30] The velocity field is

$$\begin{aligned} v_x(x,y,t)&=A\Theta(\tfrac{1}{2}-t \bmod 1)\sin(2\pi y+\phi_i),\\ v_y(x,y,t)&=A\Theta(t \bmod 1-\tfrac{1}{2})\sin(2\pi x+\phi_{i+1}), \end{aligned} \tag{12}$$

defined on a doubly periodic square domain of unit length, Θ is the Heaviside step function and A is a parameter (we use $A=0.7$), that controls the chaotic behavior of the flow. To avoid transport barriers (due to KAM tori,[17] typically present in periodically driven conservative systems) the periodicity is broken by using a random phase, ϕ_i, different in each time period.

We also consider open flow systems in which fluid continuously flows in and out a finite mixing zone. Such systems are relevant for certain chemical reactors and also in some geophysical problems. Advection in this type of open flows has been shown to be governed by a chaotic scattering type escape process generating fractal patterns of the advected tracers.[31,32]

As an example of an open flow system we use a velocity field modelling the flow around two alternately opened point-sinks in an unbounded two-dimensional domain.[33,34] The fluid particles approach the mixing zone from infinity and leave the domain through one of the sinks. The velocity field is composed by the superposition of a point-vortex and a point-sink, centered on the active sink. The complex potential corresponding to the vortex-sink is

$$w(z)=-(Q+iK)\ln|z-z_s|, \tag{13}$$

where $z=x+iy$ is the complex coordinate, z_s is the position of the sink and Q and K are the sink-strength and vortex-strength, respectively. The corresponding velocity field in polar coordinates with the origin fixed to the active sink is

$$v_r=-\frac{Q}{r}, \quad v_\phi=\frac{K}{r}, \quad r=\sqrt{(x-x_s)^2+(y-y_s)^2}. \tag{14}$$

The half distance separating the two sinks is assumed to be unity ($x_s=0, y_s=\pm 1$). The sinks are alternately opened for equal times and the period of the flow is the time unit. The inflow concentration at the boundaries of a square domain is kept constant at the value corresponding to the initial background concentration, $C(\pm 3.0,y)=C(x,\pm 3.0)=0.0$.

For both closed and open flows we integrate the advection–reaction–diffusion problem for the autocatalytic and the bistable model on a 1000×1000 lattice using a semi-Lagrangian scheme. The value of the Péclet number is $\mathrm{Pe}=1000$, and the Damköhler number is varied in a range from zero to few hundred.

III. NUMERICAL RESULTS

A. Closed flow

We find for both chemical models two distinct regimes separated by a critical Damköhler number, Da_c. The critical values are $\mathrm{Da}_c\approx 2.0$ for the autocatalytic reaction and $\mathrm{Da}_c\approx 20.0$ for the bistable model.

In the slow reaction/fast stirring regime ($\mathrm{Da}<\mathrm{Da}_c$), in both models the initial perturbation quickly decays towards a homogeneous state (Fig. 1). In the case of the autocatalytic reaction the homogenization of the perturbation is followed by a spatially uniform transition to the stable equilibrium, $C=1$, as in a reactor with initially premixed components. This is because the original uniform state is unstable, and cannot be restored by the homogenization of the perturbation, since the homogenized state still deviates slightly from the unstable equilibrium. In the bistable system the perturbation is dispersed and the system simply returns to the unperturbed initial state, $C=0$. In this regime, the chemical reaction is too slow to sustain the localized perturbation that is diluted by the strong stirring. Note that for both chemical models the final state would be the same for a spatially uniform perturbation with the same spatial mean. Thus, a coarse grained model could, at least qualitatively, reproduce the evolution of the system.

When $\mathrm{Da}>\mathrm{Da}_c$ the localized perturbation may persist and propagate in the form of a filament with a roughly constant width and rapidly increasing length (Fig. 2). This continues until the filaments cover the whole domain and finally the system becomes uniform again, $C=1$. This occurs in all cases in the autocatalytic case, but only if $\alpha<0.5$ in the bistable case. If $\alpha>0.5$ a localized perturbation in the bistable case decays. The width of the propagating filaments increases with Da. We note, that the average profile of the filament (width, amplitude) is apparently independent of the details of the initial perturbation, indicating that it is determined by the interplay between the chemical and transport

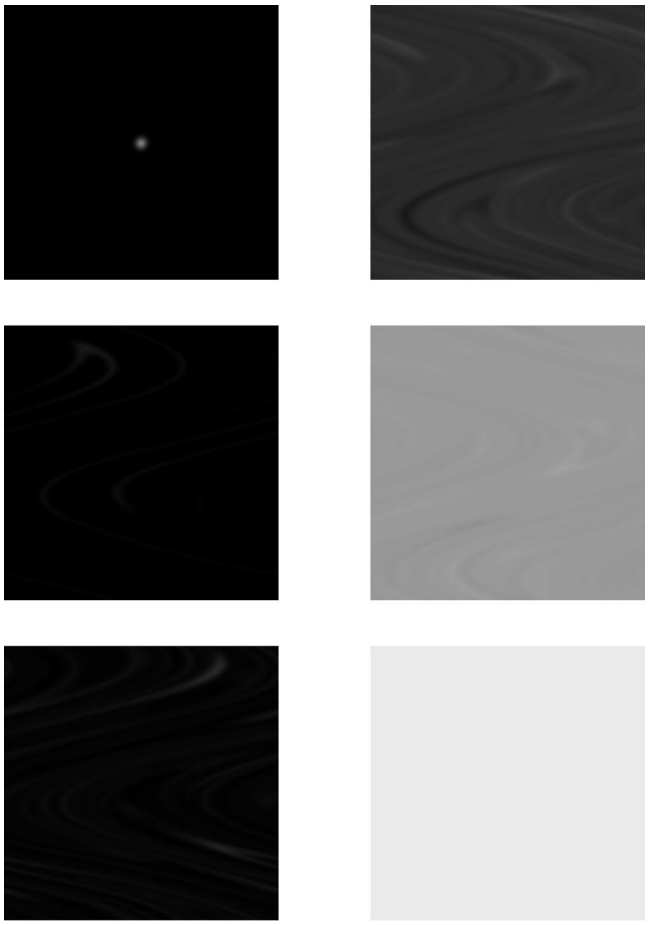

FIG. 1. Snapshots of the spatial distribution for the autocatalytic reaction for $\mathrm{Da}=1.0$ ($<\mathrm{Da}_c$) at $t=0.0$, 2.0, 4.0, 6.0, 8.0. The amplitude of the initial perturbation is chosen to be $C_0=0.5$ in order to make the initial decay visible.

dynamics in the system. In this regime the transition from the initially uniform state to the final one is strongly nonuniform in space. Since the spatial variation is essential, a coarse grained model that was unable to resolve the filaments, would produce very different outcomes.

The transition from the nonhomogeneous to homogeneous reaction in the case of the autocatalytic model for decreasing Da is clearly shown by the snapshots of the spatial distribution taken at the midpoint of the transition defined by the spatial mean concentration $\overline{C}=0.5$ (Fig. 3). To characterize the change in the nonuniformity of the reactions as Da is varied we plotted the relationship between the first and the second moments ($M_1\equiv\langle C\rangle$ and $M_2\equiv\langle C^2\rangle$) of the chemical distribution (Fig. 4). There are two extreme situations. In case of a spatially uniform system the averaging can be ignored and thus $M_2=M_1^2$. For a strongly nonuniform distribution with only two possible values 1 and 0 (representing a two-phase system with a very narrow transition zone) the square for the second moment is irrelevant and $M_2=M_1$. Figure 4 clearly shows the transition from the linear to the quadratic relationship as Da is decreased.

The time dependence of the mean concentration, $\overline{C}$ (equivalent here to the spatial average of the deviation from the initial state) is shown in Fig. 5 for different Da numbers. For large Da numbers, after an initial transient time, an exponential growth can be observed with the growth rate independent of the Damköhler number for both chemical models. This shows that the growth of the mean concentration is controlled by the stirring, that increases the length of the propagating filament. Note, that for the bistable system a localized perturbation with its spatial mean concentration

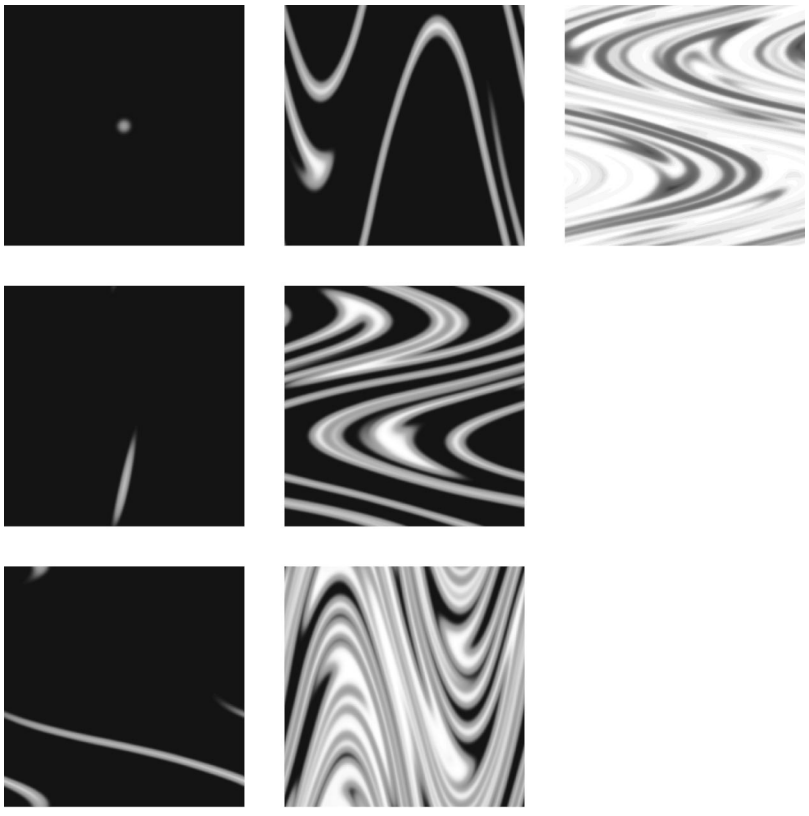

FIG. 2. Snapshots of the spatial distribution for the autocatalytic model for a supercritical Damköhler number, $\mathrm{Da}=7.0$ at $t=0.0$, 0.5, 1.0, 1.5, 2.0, 2.5, 3.0, 3.5. The amplitude of the initial perturbation is $C_0=0.5$. The bistable model shows qualitatively similar behavior.

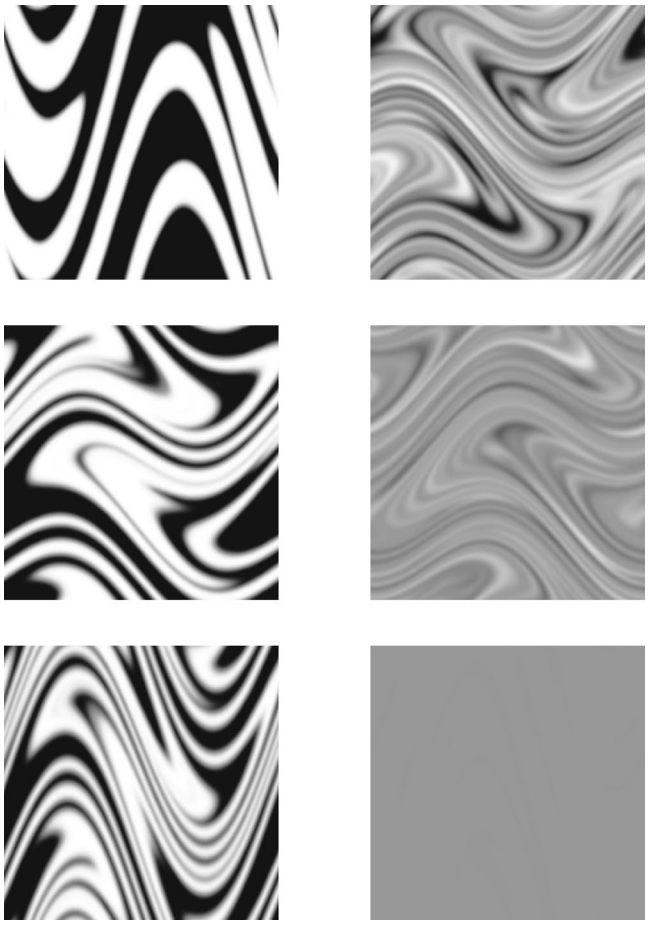

FIG. 3. Snapshots of the spatial distribution for the autocatalytic model at the midpoint of the transition [defined by $\langle C\rangle(t)=0.5$] for Da=35.0, 12.0, 8.40, 4.1, 2.9, 1.0.

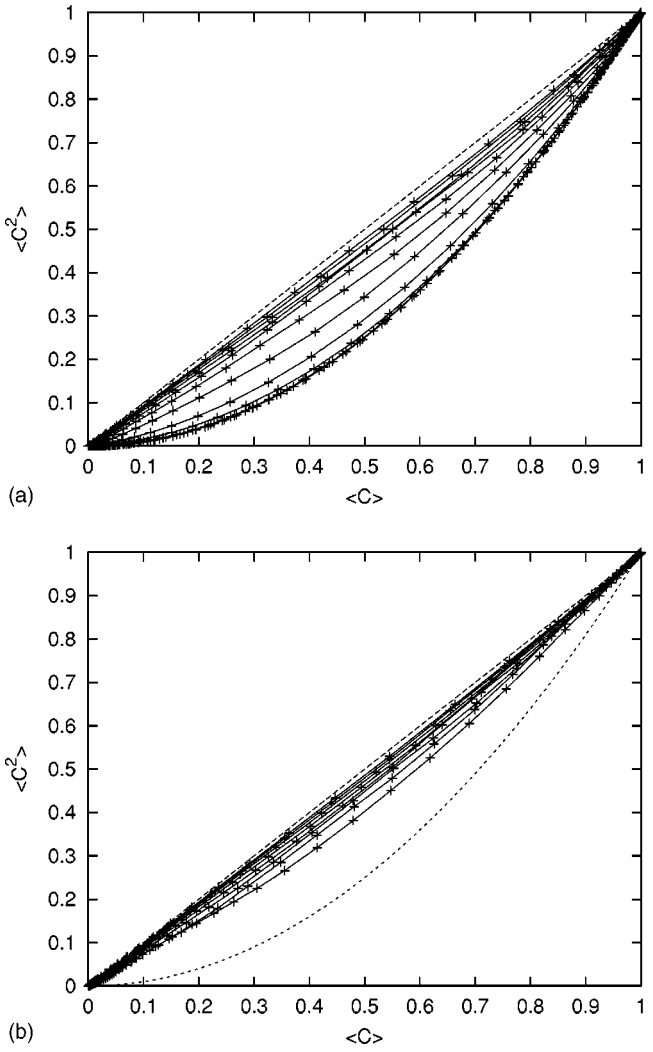

FIG. 4. The relationship between the first and the second moment of the spatial distribution for different values of Da. (a) Autocatalytic, (b) bistable.

well below the threshold, α, can flip the system to the other steady state. This is a strong example where spatial smoothing does not work.

For $\mathrm{Da}<\mathrm{Da}_c$ the homogeneous dynamics is relevant. In the bistable system the mean concentration simply decays to zero exponentially as in the homogeneous system (for $\overline{C}\ll 1$)

$$\frac{d\overline{C}}{dt}=Da\,\frac{d\mathcal{F}}{d\overline{C}}\overline{C}=-\alpha\,\mathrm{Da}\,\overline{C},\quad \overline{C}\sim e^{-\alpha\,\mathrm{Da}\,t}. \tag{15}$$

In the autocatalytic model, the growth of the mean concentration depends on the Da number. When the time dependence is plotted against $\mathrm{Da}\,t$ (Fig. 6) (i.e., the time unit is the chemical time) the curves corresponding to $\mathrm{Da}<\mathrm{Da}_c$ collapse showing that in this regime the transition is independent of the stirring rate, as expected for a spatially uniform system, and the numerical results agree well with the solution obtained for the homogeneous system (9). In this regime the two reactants (A and B) are brought close to each other by the flow at a higher rate than they can react, therefore further increase of the mixing rate cannot enhance the production. The growth of the mean concentration is limited by mixing (transport) for supercritical Damköhler numbers and limited by the chemical reaction (local dynamics) below the critical value.

B. Open flow

In the open flow case we find again a transition at a critical value of the Damköhler number.

When the stirring is strong ($\mathrm{Da}<\mathrm{Da}_c$) any localized perturbation dies out and both models return to the original state. There is no homogeneous transition for the autocatalytic system as this would be incompatible with the inflow boundary conditions. In other words, the perturbation is expelled completely from the system (through the sinks) and thus even the unstable basic state ($C=0$) can be restored.

When $\mathrm{Da}>\mathrm{Da}_c$, similarly to the closed flow case, the perturbation produces a propagating filament. However, in this case due to the continuous outflow and inflow the filament cannot fill the domain uniformly. After a short transient a nonuniform stationary state sets in, with the mixing zone partly covered by a complex filamental structure (Fig. 7). In our case the stationary pattern varies periodically with the period of the flow. For the autocatalytic model, a small am-

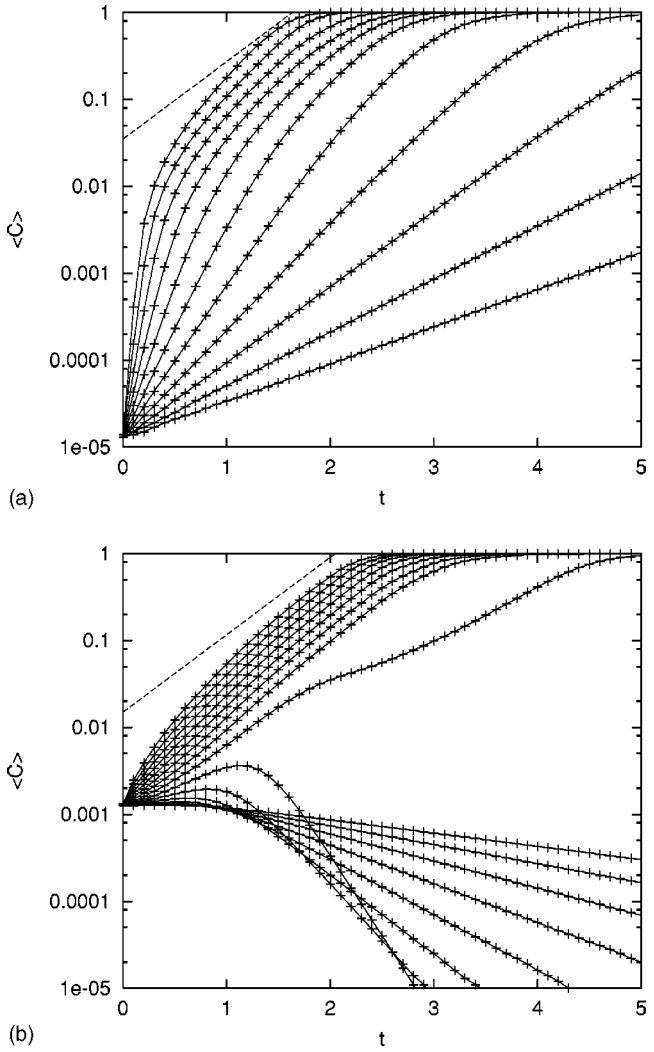

FIG. 5. The time dependence of the total concentration for different values of Da, (a) autocatalytic reaction and (b) bistable model. The dashed line indicates the rate of growth of the length of a filament due to advection.

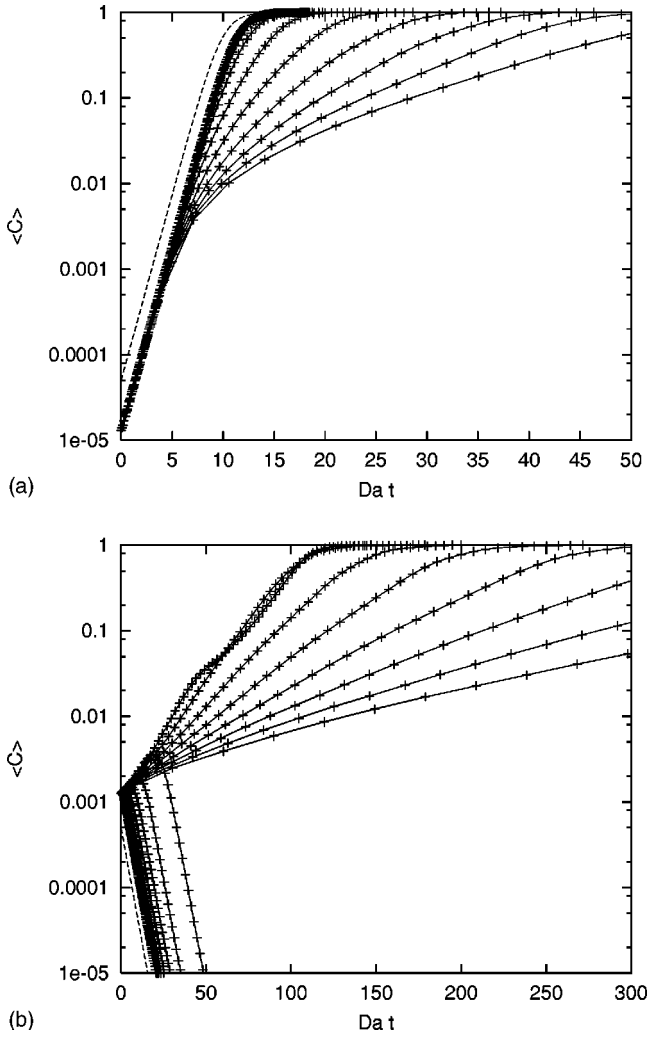

FIG. 6. Same as Fig. 5 with rescaled time. The dashed line shows the time dependence for the spatially homogeneous system.

plitude perturbation is sufficient to initiate the propagating filament, while in the bistable model only perturbations larger than the threshold, α, are able to trigger the transition to the nonuniform stationary state. (Furthermore an additional condition for the existence of the nonuniform stationary state is again that $\alpha < 0.5$.)

One can observe that the nonuniform (periodic) stationary pattern follows the fractal unstable manifold of the nonescaping set formed by fluid particles that are trapped forever in the mixing zone.[34] The unstable manifold can be easily visualized by simply following the evolution of an ensemble of fluid elements (e.g., representing a droplet of dye) advected by the flow (Fig. 8). For the autocatalytic reaction this has been already observed in a kinematic model where B particles are treated as individual tracers.[35] As in the closed flow case, the width of the filaments increases with the Da number (Fig. 9). The dependence on the Da number of the total concentration (i.e., the area covered by the filaments) in the stationary state is shown in Fig. 10. We find a continuous transition for the autocatalytic reaction ($\mathrm{Da}_c = 2.3$) and a discontinuous one for the bistable model ($\mathrm{Da}_c = 24.2$).

IV. THE LAGRANGIAN FILAMENT SLICE MODEL

Here we introduce a reduced one-dimensional model in order to explain the numerical results described in the preceding section. In the presence of chaotic transport fluid elements are stretched into elongated filaments. This is well known from numerical simulations and has been observed in laboratory experiments using dye droplets.[16,32,36] In a two-dimensional system, one can assign to any point of the flow a convergent and a divergent direction associated with the eigenvectors corresponding to the negative and positive Lyapunov exponents ($-\lambda$ and λ) of the chaotic advection. These directions are tangent to the stable and unstable foliations of the advection dynamics, respectively. Any advected material line (e.g., isocontours of a conserved tracer) tends to align along the unstable foliation in forward time, or along the stable foliation in backward time. Thus, the stirring process smooths out the concentration of the advected tracer along the stretching direction, whilst enhancing the concentration gradients in the convergent direction.

Let us now separate the original reaction–advection–diffusion problem along the (Lagrangian) stretching and convergent directions. In the stretching direction the perturbation

FIG. 7. Snapshots of the spatial distribution for the autocatalytic reaction in the open flow system for a supercritical Damköhler number, $\mathrm{Da}=14.0>\mathrm{Da}_c$ at $t=0.0$, 1.0, 2.0, 3.0, 4.0, 5.0. The distribution at $t=5.0$ has already reached the time-periodic stationary state. The amplitude of the perturbation is $C_0=0.5$. For subcritical Damköhler numbers the perturbation dies out. (The bistable model shows similar behavior but for different values of Da.)

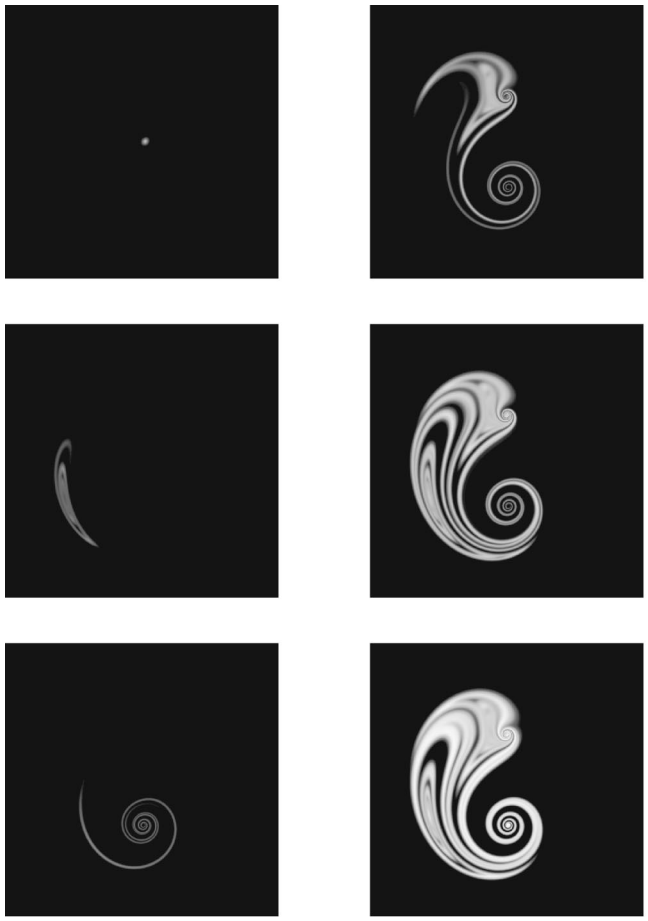

FIG. 9. Spatial distribution in the open flow for the autocatalytic model in the time-periodic stationary state for Da=70.0, 24.0, 11.8, 4.0.

is spread by advective transport, that is the dominant process being much faster than diffusion. In the convergent direction the formation of small scale structure indicates that all three processes of reaction, advection, and diffusion are important and need to be considered together. The resulting equation determines the mean transverse profile of the filament that propagates along the divergent direction following the unstable foliation.

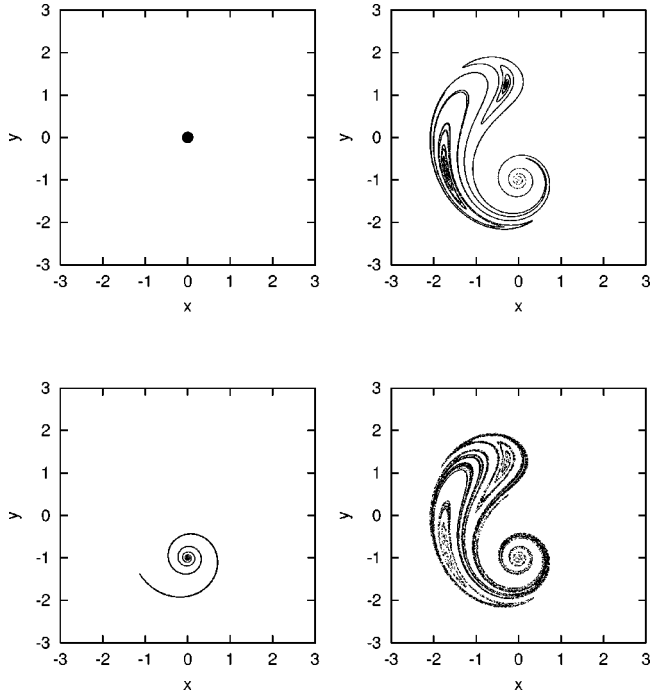

FIG. 8. The evolution of an ensemble of particles (e.g., representing a droplet of dye) in the open flow system ($t=0.0$, 2.0, 4.0, 6.0).

Thus one expects that the locus of the center of the filament can be obtained simply by advecting a material contour starting in the region of the initial perturbation. This is confirmed by the numerical simulations as shown in Fig. 11 for the closed flow model, and is consistent with Fig. 8 for the open flow system. An important difference between the two is that while in the closed flow the contour gradually fills the whole domain, in the open flow it draws out the unstable manifold of the set formed by all nonescaping orbits. The length of the contour increases exponentially (Fig. 12), $L(t)\sim\exp(\theta t)$ with $\theta\approx 2.05$. We note, that the contour lengthening rate, θ is always larger than the Lyapunov exponent (λ), which represents the average growth rate of infinitesimal line elements. This is because the instantaneous stretching rate fluctuates and the increase of the total length is dominated by the growth of a line elements that experience a faster than average stretching. In dynamical systems language the contour lengthening rate θ is given by the topological entropy[17,37,38] of the advection dynamics.

In the convergent direction we have the following one-dimensional equation for the average profile of the filament

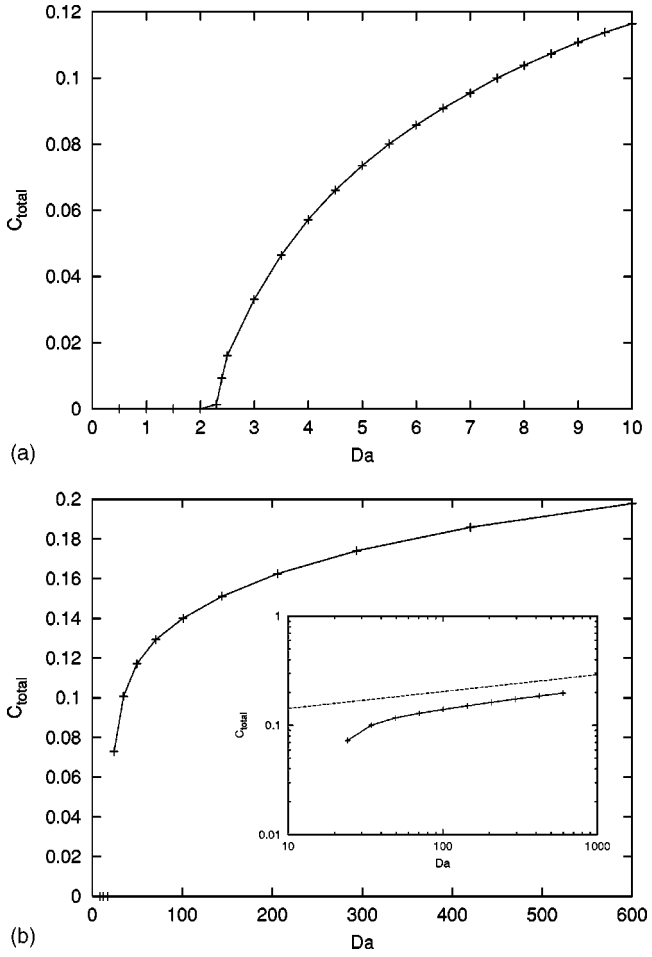

FIG. 10. The total concentration in the steady state for the open flow system as a function of the Damköhler number for the autocatalytic reaction (a) and the bistable model (b). The dashed line in the inset indicates the predicted asymptotic behavior $C_{\text{total}} \sim \text{Da}^{(2-D)/2}$ where D is the fractal dimension of the unstable foliation of the nonescaping set, $D=1.69$.

$$\frac{\partial}{\partial t}C-\lambda x\frac{\partial}{\partial x}C=k\mathcal{F}(C)+\kappa\frac{\partial^2}{\partial x^2}C, \tag{16}$$

representing the evolution of a transverse slice of the filament in a Lagrangian reference frame (i.e., following the motion of a fluid element). The second term on the left-hand side is a stretching term that takes into account the mean convergent flow and $\mathcal{F}$ is the original reaction term. The stretching term in Eq. (16) can be interpreted as advection by a pure strain flow along its convergent direction $v_x=-\lambda x$. In the two-dimensional problem the strength of stretching fluctuates in space and time. To capture the average behavior this can be represented by a constant stretching rate, λ, equal to the Lyapunov exponent of the chaotic advection. Therefore the equation above can be regarded as a Lagrangian mean field description. Equation (16) has also been studied recently by McLeod *et al.*[39] investigating the filament width of oceanic plankton distributions.

Equation (16) is defined on $-\infty<x<\infty$ with the boundary conditions

$$C(x\to\pm\infty)=0, \quad \frac{dC}{dx}(x\to\pm\infty)=0 \tag{17}$$

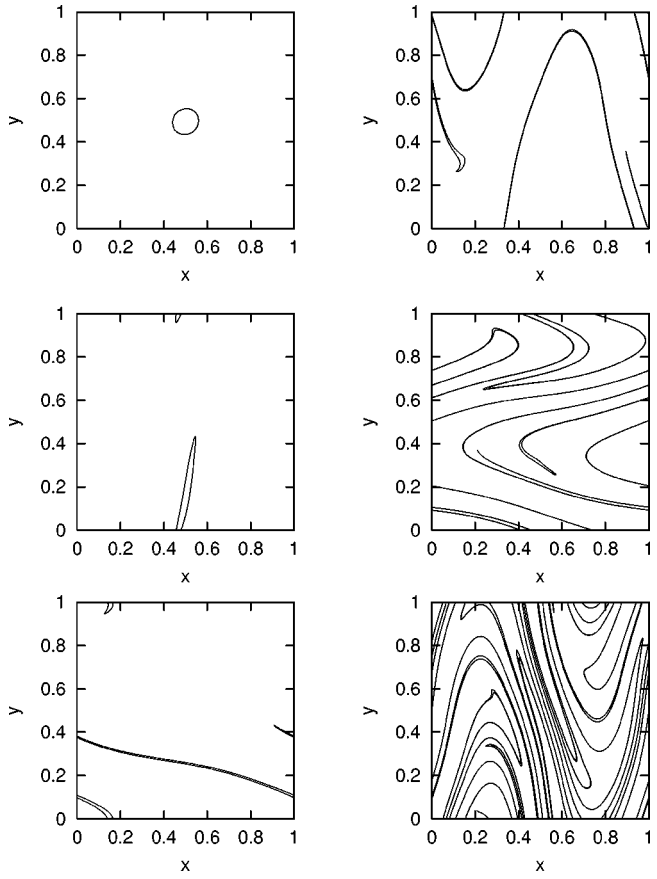

FIG. 11. Temporal evolution of a material line advected by the closed flow. The radius of the initial circular contour is $r=0.06$ and the figures correspond to $t=0.0$, 0.5, 1.0, 1.5, 2.0, 2.5 as in Fig. 2, for comparison.

representing the assumption that most of the system is in the background state, $C=0$, so that different parts of the filament are well separated from each other and they do not interact. The single filament approximation is not valid for the late stage of the evolution when the filaments can overlap.

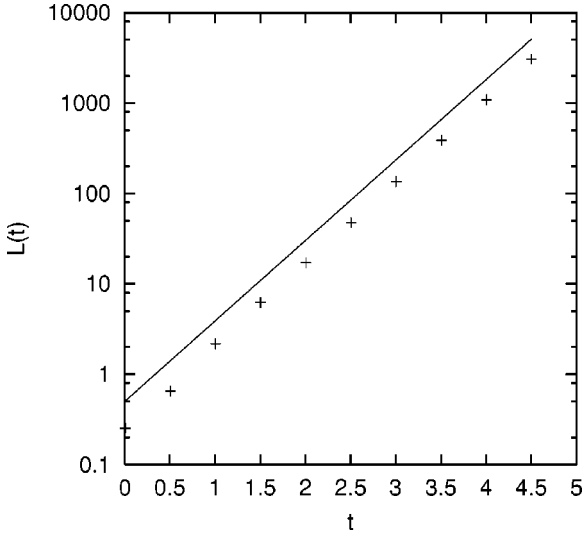

FIG. 12. The growth of the length of the contour shown in Fig. 11 as a function of time. The continuous line represents an exponential growth $\sim\exp(2.05t)$.

The homogeneous steady state, $C(x)\equiv 0$, is a trivial solution of (16) and (17). Let us now consider the evolution of a localized pulselike disturbance. (We use perturbations centred at the origin, but it turns out that the asymptotic behavior is independent of the initial position of the perturbation.)

For a nonreactive tracer ($k=0$) the equation (16) has asymptotic solutions (for large t) of the form of a Gaussian pulse whose amplitude decays exponentially in time

$$C(x,t)\sim \exp(-\lambda t)\exp\left(-\frac{x^2\lambda}{2\kappa}\right). \tag{18}$$

The width of the Gaussian, $l_{\mathrm{dif}}\equiv\sqrt{\kappa/\lambda}$, is determined by the balance between the strain and diffusion.

Let us now consider the case of a reactive tracer ($k\neq 0$) without stretching ($\lambda=0$). It is well known that reaction–diffusion systems with multiple equilibria have travelling front solutions connecting different steady states.[26,40,41] The fronts move with a constant speed v_0 with no change of shape, $C(x,t)=C(x-v_0t)$.

The reaction–diffusion problem corresponding to the autocatalytic model is known as the Fisher equation[42] (or Kolmogorov–Petrovsky–Piskunov equation[27] in the combustion literature) and describes the propagation of a stable phase ($C=1$, component B) into an unstable one ($C=0$, component A). Localized perturbations evolve into a pair of fronts moving away from the center with the asymptotic speed, $v_0=2\sqrt{k\kappa}$.

For the bistable model (11) the velocity of the front joining the two stable states, $C(x\to-\infty)=1$ and $C(x\to\infty)=0$, is[26,40,41]

$$v_0=\sqrt{k\kappa}\int_0^1 \mathcal{F}(C)dC=\sqrt{\frac{k\kappa}{2}}(1-2\alpha). \tag{19}$$

The sign of the above expression can be either positive or negative showing that the direction of the propagation depends on the parameter α. The single travelling front solution can be found analytically[26] as

$$C(x-v_0t)=\left[1+\exp\left(\frac{x-v_0t}{\sqrt{2}}\right)\right]^{-1}. \tag{20}$$

When the initial basic state is $C=0$ a localized perturbation can initiate a pair of propagating fronts moving away from each other only if $\alpha<0.5$, otherwise the direction of the front propagation is such that the fronts approach each other and the perturbation dies out. This explains the decay of the perturbations for $\alpha>0.5$ in the two-dimensional simulations independently of the stirring rate.

Thus, in the absence of stretching both type of systems have travelling front solutions with the front speed proportional to $\sqrt{k\kappa}$. A localized perturbation generates a pair of fronts moving in opposite directions away from the center. (For bistable systems this happens only if $\alpha<0.5$.) For the autocatalytic model the amplitude of the perturbation can be arbitrarily small, while it must exceed the threshold α in the bistable case.

In the presence of stretching, $\lambda>0$ one expects that the convergent flow will eventually stop the propagation of the fronts at a point $x=w$ where the speed of the propagation is balanced by the advection

$$w\lambda\approx\sqrt{k\kappa}. \tag{21}$$

This gives an estimate for the width of the resulting filament as

$$w\sim\frac{\sqrt{k\kappa}}{\lambda}=l_{\mathrm{dif}}\sqrt{\widetilde{\mathrm{Da}}},\quad \widetilde{\mathrm{Da}}\equiv\frac{k}{\lambda}, \tag{22}$$

where we have introduced the Lagrangian Damköhler number, $\widetilde{\mathrm{Da}}$. This is defined on the basis of the Lyapunov time, $1/\lambda$, of the flow, representing the Lagrangian characteristic time scale of the two-dimensional advection problem. This turns out to be more appropriate for the filamentation problem than the definition (4) based on Eulerian characteristics like the average flow velocity U.

The propagation velocity (21) is for an isolated front only. Therefore we expect that the scaling for the filament width (22) is valid when the distance between the two fronts, representing the edges of the steady filament, is sufficiently large compared to the diffusive scale, $w\gg l_{\mathrm{dif}}$, that is $\widetilde{\mathrm{Da}}\gg 1$.

Equation (16) can be nondimensionalized by using the Lyapunov time, λ^{-1}, as the time-scale unit and the diffusive scale, l_{dif}, as the unit length

$$\frac{\partial}{\partial t}C-x\frac{\partial}{\partial x}C=\widetilde{\mathrm{Da}}\,\mathcal{F}(C)+\frac{\partial^2}{\partial x^2}C. \tag{23}$$

Since the one-dimensional problem is defined on an unbounded domain, the Péclet number does not appear in (23). For the two-dimensional problem the characteristic scale of the velocity field, L, is finite and this can be used to define a Lagrangian Péclet number based on the Lyapunov exponent of the flow as

$$\widetilde{\mathrm{Pe}}\equiv\frac{L^2\lambda}{\kappa}=\left(\frac{L}{l_{\mathrm{dif}}}\right)^2. \tag{24}$$

Using this the expression for the width of the filament can be rewritten as

$$\frac{w}{L}\sim\frac{\sqrt{k\kappa}}{\lambda L}=\sqrt{\frac{\widetilde{\mathrm{Da}}}{\widetilde{\mathrm{Pe}}}}. \tag{25}$$

The straining flow approximation can only be valid for scales smaller than L ($w\ll L$), thus (25) is expected to be correct in the range $1\ll\widetilde{\mathrm{Da}}\ll\widetilde{\mathrm{Pe}}$.

In the open flow model in the stationary state the filaments cover a fractal set. For the parameter values used in our simulations the dimension of this was found to be $D\approx 1.69$. The area of the large concentration region can be obtained by using the dimensionless filament width w/L as the resolution when observing this region. Since the number of boxes of size w/L needed to cover the region is proportional to $(w/L)^{-D}$,[17] the area A of this regions is

$$\frac{A}{L^2}\sim\left(\frac{w}{L}\right)^{2-D}=\left(\frac{\widetilde{\mathrm{Da}}}{\widetilde{\mathrm{Pe}}}\right)^{(2-D)/2}. \tag{26}$$

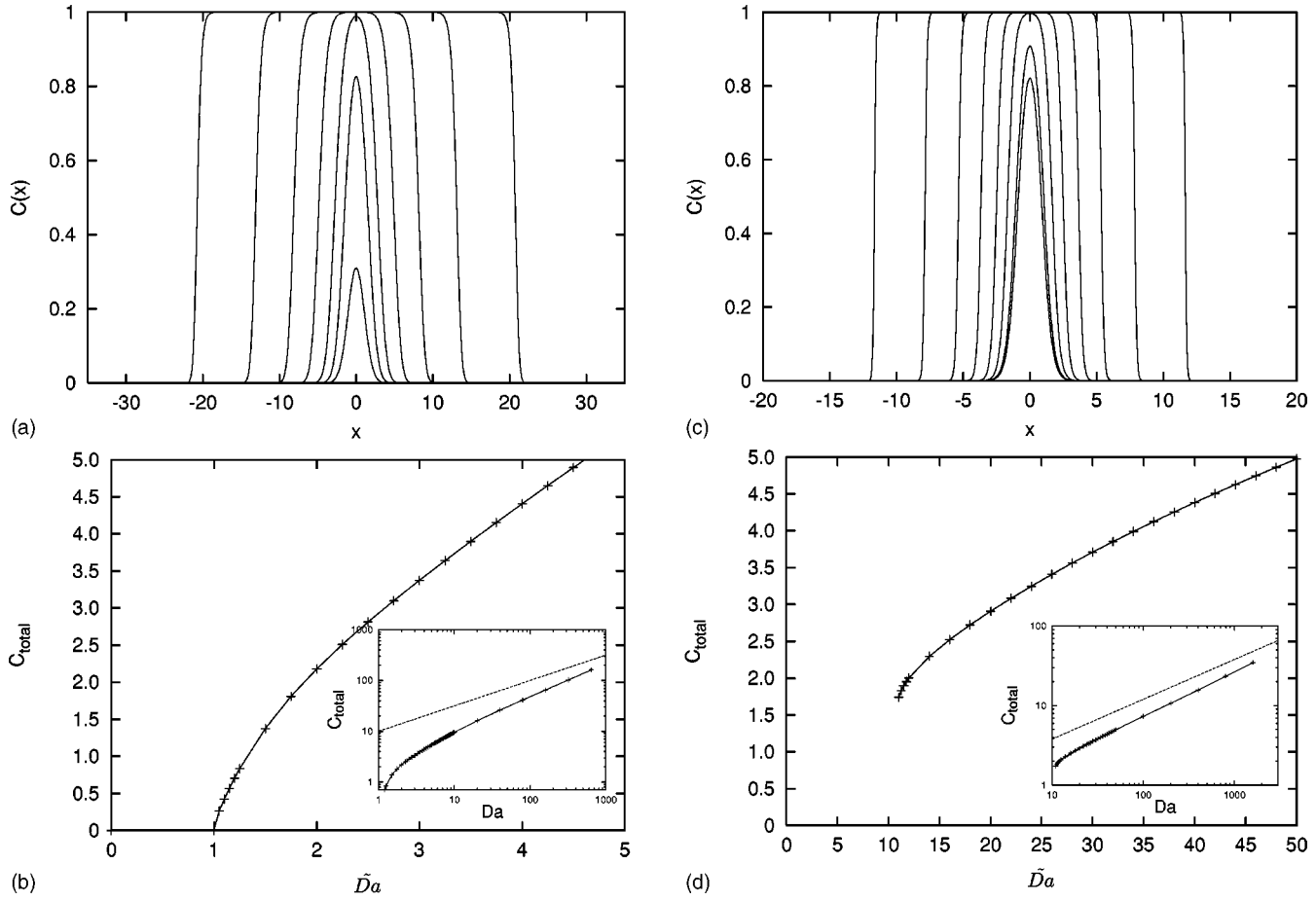

FIG. 13. Steady solutions of the one-dimensional reaction–advection–diffusion problem, for different values of the Damköhler number (a) $\widetilde{\mathrm{Da}}=80, 40, 20, 10, 5.0, 2.5, 1.25$; (c) $\widetilde{\mathrm{Da}}=800, 400, 200, 100, 50, 25, 12.5, 11.0$ and the dependence of the total concentration in the steady state as a function of $\widetilde{\mathrm{Da}}$, (a), (b) autocatalytic, (c),(d) bistable. The dashed line in the inset indicates the predicted asymptotic behavior $C_{\mathrm{total}}\sim\sqrt{\widetilde{\mathrm{Da}}}$.

This shows, that due to the overlaps the total area grows more slowly with the Damköhler number than the area of a single isolated filament. An analogous scaling has been obtained for autocatalytic reaction on an open baker map in Ref. 43.

Numerical simulations of the reduced problem (23) show that for both chemical models there is a critical value of the Damköhler number. When $\widetilde{\mathrm{Da}}>\widetilde{\mathrm{Da}}_c$ there exists a nonuniform steady solution to (23) centered on the origin (Fig. 13). Otherwise all perturbations decay and the only steady solution is the trivial one, $C(x)\equiv 0$. The width of the nonuniform steady solution increases with $\widetilde{\mathrm{Da}}$, that appears to be consistent with (22) for large Damköhler numbers. Numerical continuation of the nonuniform steady solution for decreasing $\widetilde{\mathrm{Da}}$ confirms that this solution disappears at a critical value. The transition is found to be continuous for the autocatalytic model and discontinuous for the bistable model (see Fig. 13). Let us now analyze the transition in the reduced problem (23) in more details for the two chemical models, separately.

A. Autocatalytic model

For the autocatalytic model the nonuniform solution approaches and coalesces with the uniform solution when $\widetilde{\mathrm{Da}}_c$ is approached from above. When $\widetilde{\mathrm{Da}}<\widetilde{\mathrm{Da}}_c$ localized perturbations decay, showing that the uniform state, $C(x)=0$, in spite of being an unstable fixed point of the homogeneous system is stable against localized disturbances. Thus stirring stabilizes the unstable equilibrium of the homogeneous system by dispersing and diluting the perturbation. This is consistent with the behavior observed in the two-dimensional simulations for subcritical Damköhler numbers, showing homogenization and decay of the perturbation followed by growth only after the reactants were distributed uniformly in space. For supercritical Damköhler numbers the uniform solution is unstable against localized perturbations. Arbitrarily weak perturbations are sufficient to reach the nonuniform steady state.

Just above the critical point, $\widetilde{\mathrm{Da}}-\widetilde{\mathrm{Da}}_c\ll 1$, the amplitude of the nonuniform solution is small and the chemical dynamics can be linearized about the background state

$$\frac{\partial C}{\partial t}-x\frac{\partial C}{\partial x}=\widetilde{\mathrm{Da}}\,C+\frac{\partial^2 C}{\partial x^2}. \tag{27}$$

This problem has been studied by Martin[44] in the context of plankton populations. Equation (27) has asymptotic solutions of the form

$$C(x,t)\sim e^{-x^2/2}e^{(\widetilde{\mathrm{Da}}-1)t}, \tag{28}$$

that decay in time when $\widetilde{\mathrm{Da}}<1$ and grows exponentially, moving out of the domain of validity of the linear approximation, otherwise. (The nonlinearity would eventually stop the growth.) Thus we obtain the critical value for the autocatalytic model, $\widetilde{\mathrm{Da}}_c=1$.

Close to the transition, $\widetilde{\mathrm{Da}}=1+\epsilon, 0<\epsilon\ll 1$, one can look for a steady nonuniform solution of the form

$$C(x;\epsilon)=\epsilon C_1(x)+\epsilon^2 C_2(x)+\cdots. \tag{29}$$

Substituting this into (16) for the term first order in ϵ we obtain

$$\frac{d^2C_1}{dx^2}+x\frac{dC_1}{dx}+C_1=0 \tag{30}$$

that has the solution $C_1=Ae^{-x^2/2}$, where A is a constant that can be determined from the equation for the terms second order in ϵ,

$$\frac{d^2C_2}{dx^2}+x\frac{dC_2}{dx}+C_2=C_1^2-C_1. \tag{31}$$

The left-hand side of the equation can be written as

$$\frac{d}{dx}\left(xC_2+\frac{dC_2}{dx}\right)=C_1^2-C_1. \tag{32}$$

Integrating both sides over the whole domain the left-hand side vanishes, according to (17), and an equation for the constant A is obtained

$$\int_{-\infty}^{\infty}(C_1^2-C_1)dx=A^2\sqrt{\pi}-A\sqrt{\frac{\pi}{2}}=0 \tag{33}$$

that gives $A=1/\sqrt{2}$. Thus, the steady solution close to the transition point can be approximated as

$$C(x;\epsilon)=\frac{\epsilon}{\sqrt{2}}e^{-x^2/2}+\mathcal{O}(\epsilon^2). \tag{34}$$

B. Bistable model

For the bistable case the transition at $\widetilde{\mathrm{Da}}_c$ is discontinuous. The nonuniform solution disappears with a finite amplitude far from the uniform state. The uniform solution is stable for any $\widetilde{\mathrm{Da}}$ thus small perturbations decay independently of the Damköhler number. In the supercritical regime the uniform and nonuniform stable solutions coexist suggesting the presence of a threshold for exciting the nonuniform perturbation.

To investigate the transition further let us look for steady solutions of Eq. (23),

$$\frac{d^2C}{dx^2}=-\widetilde{\mathrm{Da}}\,\mathcal{F}(C)-x\frac{dC}{dx} \tag{35}$$

that are consistent with the boundary conditions (17). Since the nonuniform steady state is symmetric about the origin it is sufficient to consider the domain $0<x<\infty$, with the constraints

$$C(x\to\infty)\to 0,\quad \frac{dC}{dx}(0)=0. \tag{36}$$

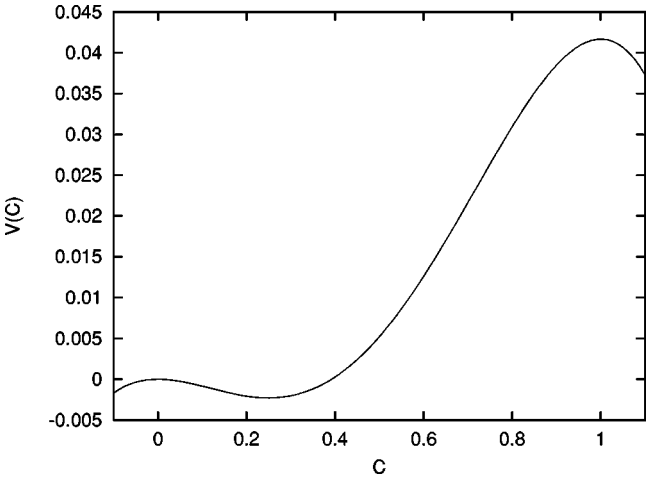

FIG. 14. The two-humped potential $V(C)$ for $\widetilde{\mathrm{Da}}=1$ and $\alpha=0.25$.

Note that, if x is interpreted as time and C as a spatial coordinate, the problem (35) is equivalent to the motion of a particle in an asymmetric two-humped potential (Fig. 14),

$$\frac{dV}{dC}\equiv\widetilde{\mathrm{Da}}\,C(\alpha-C)(C-1),$$
$$V(C)=-\widetilde{\mathrm{Da}}\,C^2\left(\frac{1}{4}C^2+\frac{(1+\alpha)}{3}C-\frac{\alpha}{2}\right), \tag{37}$$

under the effect of linear friction, with friction coefficient increasing linearly in time. The two maxima of the potential are at the stable fixed points $C=0$ and $C=1$ and the minima is at $C=\alpha$. The potential difference between the two maxima is proportional to $\widetilde{\mathrm{Da}}$. The particle trajectory satisfying (36) starts from the left slope of the higher potential hill $[\alpha<C(x=0)<1]$ with zero velocity and ends exactly on the top of the lower hill. Thus the problem reduces to finding the appropriate values of the initial coordinate, $C_0\equiv C(x=0)$. For initial conditions $C_0\in(\alpha,1)$, $C'(x=0)=0$ the trajectory of the particle may either end in the potential well $C=\alpha$ or may cross the smaller hill and escape to $-\infty$. The trajectories corresponding to the nonuniform steady solutions are at the boundary between these two types of asymptotic behavior.

We calculated numerically trajectories for a set of initial conditions in the range $C_0\in(\alpha,1)$ for a set of different values of the Damköhler number, $\widetilde{\mathrm{Da}}\in(0,40)$. The asymptotic behavior of the trajectories is indicated on the $C_0-\widetilde{\mathrm{Da}}$ plane (Fig. 15): blank, $C(x\to\infty)\to\alpha$; black, $C(x\to\infty)\to-\infty$. The required steady solutions are on the boundary of the two regions. The numerical results show that for small $\widetilde{\mathrm{Da}}$ there is no such boundary and a solution of the type (36) does not exist. In the particle analogy the interpretation of this is that the difference in the height of the two hills is not sufficiently large to compensate for the energy dissipated by friction, thus the particles cannot escape. When $\widetilde{\mathrm{Da}}$ is increased above the critical value $\widetilde{\mathrm{Da}}_c$ there are two solutions. If the hill at $C=1$ is high enough there are initial conditions for which the particles have sufficient energy to cross the potential barrier. Clearly, particles with initial conditions below the height of the lower potential hill are still trapped in the potential

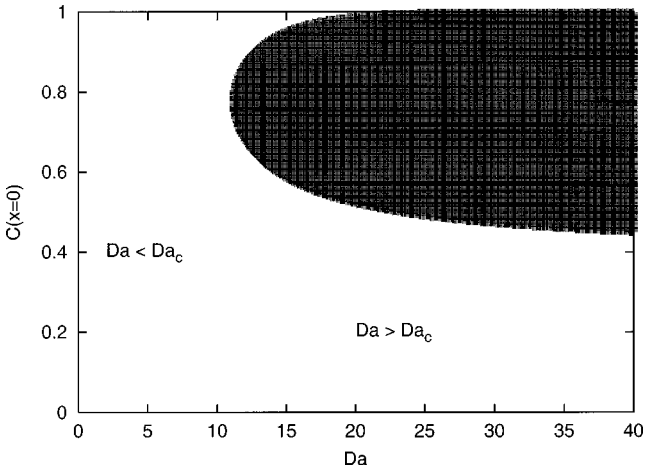

FIG. 15. The shaded area shows initial conditions resulting in the escape of the particle from the potential well. The boundary of the shaded area corresponds to the steady filaments solutions. Note, that the filament solution disappears for subcritical Damköhler numbers ($\widetilde{\mathrm{Da}}=11.0$).

well. Also, particles started from a point very close to the top of the higher hill are unable to escape since they may spend very long time in the neighborhood of the stationary point and go through the potential well at a late time when the friction is strong. Thus, for $\widetilde{\mathrm{Da}}<\widetilde{\mathrm{Da}}_c$ the initial conditions C_0^{escape} for which particles escape to infinity are in an the interval of the form

$$\alpha<C_{0,1}(\widetilde{\mathrm{Da}})\leqslant C_0^{\mathrm{escape}}\leqslant C_{0,2}(\widetilde{\mathrm{Da}})<1, \tag{38}$$

where $C_{0,1}(\widetilde{\mathrm{Da}})$ are $C_{0,2}(\widetilde{\mathrm{Da}})$ are initial conditions corresponding to steady nonuniform solutions of (16). As the Damköhler number is decreased the two solutions approach each other and disappear at $\widetilde{\mathrm{Da}}_c=11.0$.

The trajectory starting from $C(x=0)=C_{0,2}(\widetilde{\mathrm{Da}})$ clearly corresponds to the steady nonuniform solution found in the numerical simulations of the time-dependent problem. The solution corresponding to the lower branch, $C(x=0)=C_{0,1}(\widetilde{\mathrm{Da}})$, however, is not found as an attractor of the time-dependent problem. This suggests that this is an unstable solution playing the role of a threshold separating the basins of attraction of the uniform and non-uniform stable solutions. [It can be shown that all initial conditions that are above (below) this separating solution everywhere, converge to the nonuniform (uniform) steady state. This, of course, does not say anything about initial conditions partly below and partly above the separating solution.]

V. SUMMARY AND DISCUSSION

The one-dimensional Lagrangian filament model (16) clearly explains the qualitative features of the two-dimensional numerical results. It shows how a steady filament profile can arise as a result of the interaction between the propagation of a reaction–diffusion front and stretching due to chaotic advection. The disappearance of the filament type solution for subcritical Damköhler numbers explains the transition observed in the two-dimensional simulations. The advective propagation of the filament along the unstable foliation of the chaotic advection explains the exponential growth of the mean concentration. In principle, these results could be used as a numerical technique for obtaining the approximate spatial distribution of the chemical components by combining a two-dimensional contour–advection calculation with the information about the filament width obtained from the steady solution of the one-dimensional model.

TABLE I. The critical values of the Lagrangian Damköhler number for the two-dimensional simulations and for the one-dimensional single filament model

	Closed	Open	1D model
Autocatalytic	≈ 1.2	1.05	1.0
Bistable	≈ 12.0	11.06	11.0

In order to compare the critical Damköhler numbers predicted by the one-dimensional mean strain model with the ones obtained from the direct numerical simulations we calculate the Lagrangian Damköhler numbers corresponding to the two-dimensional problem. The Lyapunov exponents of the advection in the two model flows was found to be $\lambda_{\mathrm{closed}}\approx 1.66$ and $\lambda_{\mathrm{open}}\approx 2.19$. The critical values of the Lagrangian Damköhler number based on these Lyapunov exponents are presented in Table I and show a very good agreement.

In our analysis we neglected the fluctuations of the stretching rate. In reality there is a distribution of stretching rates. The effect of this is visible in the numerical simulations showing that the width of the filament slightly fluctuates in space and time. Also the direction of the stretching fluctuates and foldings of the filament may lead to large curvatures whose effect is not captured by our one-dimensional description. Another effect is the nonuniform density of the unstable foliation pointed out by Alvarez *et al.*[38] Thus the advected filament can overlap with itself well before it fills the whole domain. Some regions of the flow are filled while others are still empty.

Here we investigated only reactive systems described by the distribution of a single species. We expect, however, that the basic phenomena described in this paper remain valid for multicomponent reactive systems that may have a number of different chemical time scales. One example of this type is the case of excitable systems[26,41,45] under stirring by a chaotic flow discussed in Ref. 46. Excitable systems have two different time scales corresponding to fast and slow components. Although these systems only have a single (stable) steady state, the rest state, they also have a metastable excited state that persists for a finite time only. Excitable systems under stirring exhibit similar behavior to the one presented here, including advective propagation in form of a steady excited filament and the existence of a critical Damköhler number. The one-dimensional excitable reaction–diffusion systems have travelling pulse solutions, that in the presence of stretching leads to the appearance of a steady excited filament solution. This can be simple unimodal, as in our case, but it can also have a bimodal structure with the central part of the filament returned to the rest state. Thus the existence of an extra chemical time scale in this system allows for somewhat more complex structures and a

further transition in the large Da number range, being a transition from coherent to noncoherent excitation of the system.

A nice example of an advectively propagating perturbation, of the kind described in this paper, has been observed recently in a so-called ocean fertilization experiment,[47] where the injection of a trace element affecting the plankton ecosystem triggered a phytoplankton bloom in the form of an elongated filament, observed on satellite images. The response of plankton ecosystem models to such perturbation in the presence of stirring has been studied in Ref. 48. We suggest that similar phenomena could also be investigated in laboratory experiments.

ACKNOWLEDGMENTS

This work was supported by the UK Natural Environment Research Council (NERC UTLS Ozone grant NER/T/S/1999/00103) and by the Hungarian Research Foundation (OTKA T032423) and the MTA-OTKA-NSF Fund (No. 526).

[1] A. Rovinsky and M. Menzinger, Phys. Rev. Lett. **69**, 1193 (1992).
[2] I. R. Epstein, Nature (London) **374**, 321 (1995).
[3] G. Metcalfe and J. M. Ottino, Phys. Rev. Lett. **72**, 2875 (1994).
[4] M. A. Allen, J. Brindley, J. Merkin, and M. J. Pilling, Phys. Rev. E **54**, 2140 (1996).
[5] R. Reigada, F. Sagués, I. M. Sokolov, J. M. Sancho, and A. Blumen, Phys. Rev. Lett. **78**, 741 (1997).
[6] E. R. Abraham, Nature (London) **391**, 577 (1998).
[7] G. Károlyi, Á. Péntek, I. Scheuring, T. Tél, and Z. Toroczkai, Proc. Natl. Acad. Sci. U.S.A. **97**, 13661 (2000).
[8] W. R. Young, A. J. Roberts, and G. Stuhne, Nature (London) **412**, 328 (2001).
[9] T. Poinsot and D. Veynante, *Theoretical and Numerical Combustion* (Edwards, New York, 2001).
[10] S. Edouard, B. Legras, F. Lefévre, and R. Eymard, Nature (London) **384**, 444 (1996).
[11] P. H. Haynes, ''Transport, stirring and mixing in the atmosphere,'' in *Mixing: Chaos and Turbulence*, edited by H. Chaté and E. Villermaux (Kluwer, Dordretch, 1999).
[12] J. H. Steele and E. W. Henderson, J. Plankton Res. **14**, 157 (1992).
[13] J. E. Truscott and J. Brindley, Philos. Trans. R. Soc. London, Ser. A **347**, 703 (1994).
[14] H. Aref, J. Fluid Mech. **143**, 1 (1984).
[15] J. M. Ottino, *The Kinematics of Mixing: Stretching, Chaos and Transport* (Cambridge University Press, Cambridge, 1989).
[16] J. M. Ottino, C. W. Leong, H. Rising, and P. D. Swanson, Nature (London) **333**, 419 (1988).
[17] E. Ott, *Chaos in Dynamical Systems* (Cambridge University Press, Cambridge, 1993).
[18] G. Z. Damköhler, Z. Elektrochem. Angew. Phys. Chem. **42**, 846 (1936).
[19] O. Paireau and P. Tabeling, Phys. Rev. E **56**, 2287 (1997).
[20] M. Chertkov, Phys. Fluids **10**, 3017 (1998).
[21] M. Chertkov, Phys. Fluids **11**, 2257 (1999).
[22] Z. Neufeld, C. López, and P. H. Haynes, Phys. Rev. Lett. **82**, 2606 (1999).
[23] Z. Neufeld, C. Lopez, E. Hernandez-Garcia, and T. Tél, Phys. Rev. E **61**, 3857 (2000).
[24] P. Yang and G. Brasseur, Geophys. Res. Lett. **28**, 717 (2001).
[25] H. Malchow, Proc. R. Soc. London, Ser. B **251**, 103 (1993).
[26] J. D. Murray, *Mathematical Biology* (Springer, New York, 1993).
[27] A. Kolmogorov, I. Petrovsky, and N. Piskunov, Bull. Univ. Moskou Ser. Int. Se. A **1**, 1 (1937).
[28] P. Constantin, A. Kiselev, A. Oberman, and L. Ryzhik, Arch. Ration. Mech. Anal. **154**, 53 (2000).
[29] F. Városi, T. M. Antonsen, and E. Ott, Phys. Fluids A **3**, 1017 (1991).
[30] R. T. Pierrehumbert, Chaos, Solitons Fractals **4**, 1091 (1994).
[31] E. Ziemniak, C. Jung, and T. Tél, Physica D **76**, 123 (1994).
[32] J. C. Sommerer, H. C. Ku, and H. E. Gilreath, Phys. Rev. Lett. **77**, 5055 (1996).
[33] H. Aref, S. W. Jones, S. Mofina, and I. Zawadski, Physica D **37**, 423 (1989).
[34] G. Károlyi and T. Tél, Phys. Rep. **290**, 125 (1997).
[35] Z. Toroczkai, Gy. Károlyi, Á. Péntek, T. Tél, and C. Grebogi, Phys. Rev. Lett. **80**, 500 (1998); Gy. Károlyi, Á. Péntek, Z. Toroczkai, T. Tél, and C. Grebogi, Phys. Rev. E **59**, 5468 (1999).
[36] W. L. Chien, H. Rising, and J. M. Ottino, J. Fluid Mech. **170**, 355 (1986).
[37] S. Newhouse and T. Pignataro, J. Stat. Phys. **72**, 1331 (1993).
[38] M. M. Alvarez *et al.*, Phys. Rev. Lett. **81**, 3395 (1998).
[39] P. McLeod, A. P. Martin, and K. J. Richards (unpublished).
[40] A. Scott, *Nonlinear Science* (Oxford University Press, Oxford, UK, 1999).
[41] J. Keener and J. Sneyd, *Mathematical Physiology* (Springer, New York, 1998).
[42] R. A. Fisher, Ann. Eugenics **7**, 355 (1937).
[43] Z. Toroczkai, G. Károlyi, Á. Péntek, and T. Tél, J. Phys. A **34**, 5215 (2001).
[44] A. P. Martin, J. Plankton Res. **22**, 597 (2000).
[45] E. Meron, Phys. Rep. **218**, 1 (1992).
[46] Z. Neufeld, Phys. Rev. Lett. **87**, 108301 (2001).
[47] E. R. Abraham *et al.*, Nature (London) **407**, 727 (2000).
[48] Z. Neufeld, P. H. Haynes, V. Garcon, and J. Sudre, Geophys. Res. Lett. (in press).